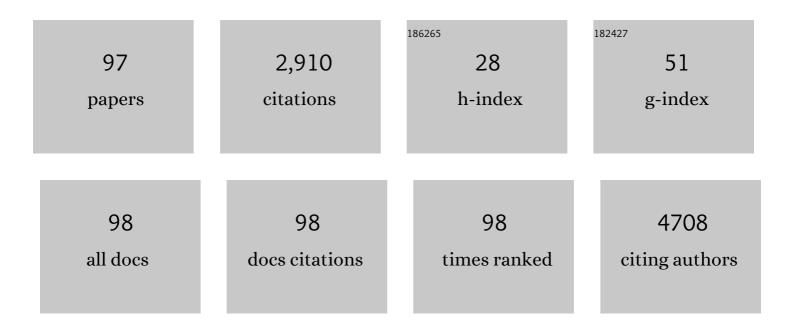
## Suk-Ho Choi

List of Publications by Year in descending order

Source: https://exaly.com/author-pdf/1216143/publications.pdf Version: 2024-02-01



SUK-HO CHOL

#	Article	IF	CITATIONS
1	Anomalous Behaviors of Visible Luminescence from Graphene Quantum Dots: Interplay between Size and Shape. ACS Nano, 2012, 6, 8203-8208.	14.6	563
2	High photoresponsivity in an all-graphene p–n vertical junction photodetector. Nature Communications, 2014, 5, 3249.	12.8	161
3	Plasmon-Enhanced Ultraviolet Photoluminescence from Hybrid Structures of Graphene/ZnO Films. Physical Review Letters, 2010, 105, 127403.	7.8	127
4	High-performance graphene-quantum-dot photodetectors. Scientific Reports, 2014, 4, 5603.	3.3	123
5	Near-Ultraviolet-Sensitive Graphene/Porous Silicon Photodetectors. ACS Applied Materials & Interfaces, 2014, 6, 20880-20886.	8.0	84
6	Graphene transparent conductive electrodes doped with graphene quantum dots-mixed silver nanowires for highly-flexible organic solar cells. Journal of Alloys and Compounds, 2018, 744, 1-6.	5.5	68
7	Graphene-Based Semiconductor Heterostructures for Photodetectors. Micromachines, 2018, 9, 350.	2.9	68
8	Semitransparent Flexible Organic Solar Cells Employing Doped-Graphene Layers as Anode and Cathode Electrodes. ACS Applied Materials & Interfaces, 2018, 10, 3596-3601.	8.0	67
9	Size-dependence of Raman scattering from graphene quantum dots: Interplay between shape and thickness. Applied Physics Letters, 2013, 102, .	3.3	63
10	Graphene p–n Vertical Tunneling Diodes. ACS Nano, 2013, 7, 5168-5174.	14.6	61
11	Highly efficient CH 3 NH 3 PbI 3 perovskite solar cells prepared by AuCl 3 -doped graphene transparent conducting electrodes. Chemical Engineering Journal, 2017, 323, 153-159.	12.7	61
12	Rapid-thermal-annealing surface treatment for restoring the intrinsic properties of graphene field-effect transistors. Nanotechnology, 2013, 24, 405301.	2.6	56
13	Graphene/Siâ€Quantumâ€Dot Heterojunction Diodes Showing High Photosensitivity Compatible with Quantum Confinement Effect. Advanced Materials, 2015, 27, 2614-2620.	21.0	56
14	Graphene/porous silicon Schottky-junction solar cells. Journal of Alloys and Compounds, 2017, 715, 291-296.	5.5	53
15	Nonvolatile-Memory Characteristics of \$hbox{AlO}^{-}\$ -Implanted \$hbox{Al}_{2}hbox{O}_{3}\$. IEEE Electron Device Letters, 2009, 30, 837-839.	3.9	50
16	Optical properties of thermally annealed hafnium oxide and their correlation with structural change. Journal of Applied Physics, 2008, 104, .	2.5	48
17	Graphene/Si-nanowire heterostructure molecular sensors. Scientific Reports, 2014, 4, 5384.	3.3	47
18	Microstructure, optical property, and electronic band structure of cuprous oxide thin films. Journal of Applied Physics, 2011, 110, .	2.5	45

#	Article	IF	CITATIONS
19	Dimensionally Engineered Perovskite Heterostructure for Photovoltaic and Optoelectronic Applications. Advanced Energy Materials, 2019, 9, 1902470.	19.5	40
20	Recent Studies of Semitransparent Solar Cells. Coatings, 2018, 8, 329.	2.6	39
21	Lamination-produced semi-transparent/flexible perovskite solar cells with doped-graphene anode and cathode. Journal of Alloys and Compounds, 2019, 775, 905-911.	5.5	38
22	Doping- and size-dependent photovoltaic properties of p-type Si-quantum-dot heterojunction solar cells: correlation with photoluminescence. Applied Physics Letters, 2010, 97, 072108.	3.3	34
23	Enhanced ultraviolet emission from hybrid structures of single-walled carbon nanotubes/ZnO films. Applied Physics Letters, 2009, 94, 213113.	3.3	32
24	Energy transfer from an individual silica nanoparticle to graphene quantum dots and resulting enhancement of photodetector responsivity. Scientific Reports, 2016, 6, 27145.	3.3	32
25	Enhancement of efficiency in graphene/porous silicon solar cells by co-doping graphene with gold nanoparticles and bis(trifluoromethanesulfonyl)-amide. Journal of Materials Chemistry C, 2017, 5, 9005-9011.	5.5	32
26	Enhanced Flexibility and Stability in Perovskite Photodiode–Solar Cell Nanosystem Using MoS <sub>2</sub> Electron-Transport Layer. ACS Applied Materials & Interfaces, 2020, 12, 4586-4593.	8.0	32
27	Graphene-Assisted Chemical Etching of Silicon Using Anodic Aluminum Oxides as Patterning Templates. ACS Applied Materials & Interfaces, 2015, 7, 24242-24246.	8.0	30
28	Enhancement of Stability of Inverted Flexible Perovskite Solar Cells by Employing Graphene-Quantum-Dots Hole Transport Layer and Graphene Transparent Electrode Codoped with Gold Nanoparticles and Bis(trifluoromethanesulfonyl)amide. ACS Sustainable Chemistry and Engineering, 2019, 7, 13178-13185.	6.7	29
29	Self-powered and flexible perovskite photodiode/solar cell bifunctional devices with MoS2 hole transport layer. Applied Surface Science, 2020, 514, 145880.	6.1	29
30	Enhancement of Memory Performance Using Doubly Stacked Si-Nanocrystal Floating Gates Prepared by Ion Beam Sputtering in UHV. IEEE Transactions on Electron Devices, 2007, 54, 359-362.	3.0	28
31	Highly-flexible graphene transparent conductive electrode/perovskite solar cells with graphene quantum dots-doped PCBM electron transport layer. Dyes and Pigments, 2019, 170, 107630.	3.7	28
32	Size-dependent radiative decay processes in graphene quantum dots. Applied Physics Letters, 2012, 101, .	3.3	27
33	Growth of two-dimensional Janus MoSSe by a single in situ process without initial or follow-up treatments. NPG Asia Materials, 2022, 14, .	7.9	27
34	Enhancement of efficiency and stability in organic solar cells by employing MoS2 transport layer, graphene electrode, and graphene quantum dots-added active layer. Applied Surface Science, 2021, 538, 148155.	6.1	26
35	Degradation reduction and stability enhancement of p-type graphene by RhCl3 doping. Journal of Alloys and Compounds, 2015, 621, 1-6.	5.5	25
36	Effect of layer number on flexible perovskite solar cells employing multiple layers of graphene as transparent conductive electrodes. Journal of Alloys and Compounds, 2018, 744, 404-411.	5.5	25

#	Article	IF	CITATIONS
37	Enhancement of the effectiveness of graphene as a transparent conductive electrode by AgNO <sub>3</sub> doping. Nanotechnology, 2014, 25, 125701.	2.6	23
38	Effect of layer number and metal-chloride dopant on multiple layers of graphene/porous Si solar cells. Journal of Applied Physics, 2018, 123, 123101.	2.5	22
39	Use of Graphene for Solar Cells. Journal of the Korean Physical Society, 2018, 72, 1442-1453.	0.7	21
40	High-Performance <i>n-i-p-</i> Type Perovskite Photodetectors Employing Graphene-Transparent Conductive Electrodes N-Type Doped with Amine Group Molecules. ACS Sustainable Chemistry and Engineering, 2019, 7, 734-739.	6.7	21
41	Highly-flexible and -stable deep-ultraviolet photodiodes made of graphene quantum dots sandwiched between graphene layers. Dyes and Pigments, 2019, 163, 238-242.	3.7	21
42	All-two-dimensional semitransparent and flexible photodetectors employing graphene/MoS2/graphene vertical heterostructures. Journal of Alloys and Compounds, 2021, 864, 158118.	5.5	21
43	Enhancement of efficiency and long-term stability in graphene/Si-quantum-dot heterojunction photodetectors by employing bis(trifluoromethanesulfonyl)-amide as a dopant for graphene. Journal of Materials Chemistry C, 2017, 5, 12737-12743.	5.5	20
44	Light-induced negative differential resistance in graphene/Si-quantum-dot tunneling diodes. Scientific Reports, 2016, 6, 30669.	3.3	19
45	Precise and selective sensing of DNA-DNA hybridization by graphene/Si-nanowires diode-type biosensors. Scientific Reports, 2016, 6, 31984.	3.3	19
46	Graphene-based vertical-junction diodes and applications. Journal of the Korean Physical Society, 2017, 71, 311-318.	0.7	17
47	Graphene/Si solar cells employing triethylenetetramine dopant and polymethylmethacrylate antireflection layer. Applied Surface Science, 2018, 433, 181-187.	6.1	17
48	Porous silicon solar cells with 13.66% efficiency achieved by employing graphene-quantum-dots interfacial layer, doped-graphene electrode, and bathocuproine back-surface passivation layer. Journal of Alloys and Compounds, 2021, 877, 160311.	5.5	17
49	High-Detectivity/-Speed Flexible and Self-Powered Graphene Quantum Dots/Perovskite Photodiodes. ACS Sustainable Chemistry and Engineering, 2019, 7, 19961-19968.	6.7	16
50	Performance enhancement of graphene/porous Si solar cells by employing layer-controlled MoS2. Applied Surface Science, 2020, 532, 147460.	6.1	16
51	High-speed heterojunction photodiodes made of single- or multiple-layer MoS2 directly-grown on Si quantum dots. Journal of Alloys and Compounds, 2020, 820, 153074.	5.5	14
52	Highly-flexible perovskite photodiodes employing doped multilayer-graphene transparent conductive electrodes. Nanotechnology, 2018, 29, 425203.	2.6	13
53	High-efficient ultraviolet emission in phonon-reduced ZnO films: The role of germanium. Journal of Applied Physics, 2008, 103, .	2.5	12
54	Nonvolatile memories of Ge nanodots self-assembled by depositing ultrasmall amount Ge on SiO2 at room temperature. Applied Physics Letters, 2008, 92, 093124.	3.3	11

#	Article	IF	CITATIONS
55	Nonvolatile memories using deep traps formed in Al2O3 by metal ion implantation. Applied Physics Letters, 2009, 94, 112110.	3.3	11
56	Formation characteristics and photoluminescence of Ge nanocrystals in HfO2. Journal of Applied Physics, 2009, 105, .	2.5	11
57	Significantly-enhanced Stabilities in Flexible Hybrid Organic-Inorganic Perovskite Resistive Random Access Memories by Employing Multilayer Graphene Transparent Conductive Electrodes. Journal of the Korean Physical Society, 2018, 73, 934-939.	0.7	11
58	Remarkable enhancement of stability in high-efficiency Si-quantum-dot heterojunction solar cells by employing bis(trifluoromethanesulfonyl)-amide as a dopant for graphene transparent conductive electrodes. Journal of Alloys and Compounds, 2019, 773, 913-918.	5.5	11
59	Anisotropic Terahertz Emission from Bi2Se3 Thin Films with Inclined Crystal Planes. Nanoscale Research Letters, 2015, 10, 489.	5.7	10
60	Highly-stable and -flexible graphene/(CF3SO2)2NH/graphene transparent conductive electrodes for organic solar cells. Nanotechnology, 2017, 28, 425203.	2.6	10
61	High-Performance Conducting Polymer/Si Nanowires Hybrid Solar Cells Using Multilayer-Graphene Transparent Conductive Electrode and Back Surface Passivation Layer. ACS Sustainable Chemistry and Engineering, 2018, 6, 12446-12452.	6.7	10
62	Graphene-nanomesh transparent conductive electrode/porous-Si Schottky-junction solar cells. Journal of Alloys and Compounds, 2019, 803, 958-963.	5.5	10
63	InAs on GaAs Photodetectors Using Thin InAlAs Graded Buffers and Their Application to Exceeding Short-Wave Infrared Imaging at 300 K. Scientific Reports, 2019, 9, 12875.	3.3	10
64	Photostable electron-transport-layer-free flexible graphene quantum dots/perovskite solar cells by employing bathocuproine interlayer. Journal of Alloys and Compounds, 2021, 886, 161355.	5.5	10
65	Effect of (O, As) dual implantation on p-type doping of ZnO films. Journal of Applied Physics, 2011, 110, 103708.	2.5	9
66	Formation of threeâ€dimensional GaAs microstructures by combination of wet and metalâ€assisted chemical etching. Physica Status Solidi - Rapid Research Letters, 2014, 8, 345-348.	2.4	9
67	Effect of nitrogen doping on the structural and the optical variations of graphene quantum dots by using hydrazine treatment. Journal of the Korean Physical Society, 2015, 67, 746-751.	0.7	9
68	Nonvolatile memories by using charge traps in silicon-rich oxides. Journal of Applied Physics, 2010, 108, 033708.	2.5	8
69	Graded-size Si-nanocrystal-multilayer solar cells. Journal of Applied Physics, 2012, 112, .	2.5	8
70	Self-powered Ag-nanowires-doped graphene/Si quantum dots/Si heterojunction photodetectors. Journal of Alloys and Compounds, 2018, 758, 32-37.	5.5	8
71	High-performance and -stability graphene quantum dots-mixed conducting polymer/porous Si hybrid solar cells with titanium oxide passivation layer. Nanotechnology, 2020, 31, 095202.	2.6	8
72	Optical Sensing Properties of ZnO Nanoparticles Prepared by Spray Pyrolysis. Journal of Nanoscience and Nanotechnology, 2019, 19, 1048-1051.	0.9	7

#	Article	IF	CITATIONS
73	High-detectivity and -stability multilayer-graphene/Si-quantum-dot photodetectors with TiOx back-surface passivation layer. Dyes and Pigments, 2019, 170, 107587.	3.7	7
74	High trap density and long retention time from self-assembled amorphous Si nanocluster floating gate nonvolatile memory. Applied Physics Letters, 2006, 89, 243513.	3.3	6
75	Effect of Ga doping concentration on the luminescence efficiency of GaN light-emitting diodes with Ga-doped ZnO contacts. Applied Physics B: Lasers and Optics, 2012, 109, 283-287.	2.2	6
76	High-Quality 100 nm Thick InSb Films Grown on GaAs(001) Substrates with an In <sub><i>x</i></sub> Al <sub>1–<i>x</i></sub> Sb Continuously Graded Buffer Layer. ACS Omega, 2018, 3, 14562-14566.	3.5	5
77	Photovoltaic and luminescence properties of Sb- and P-doped Si quantum dots. Journal of the Korean Physical Society, 2012, 60, 1616-1619.	0.7	4
78	In-situ monitoring of AuCl3-doping and -dedoping behaviors in graphene. Journal of the Korean Physical Society, 2014, 64, 1327-1330.	0.7	4
79	Successful Fabrication of <scp>GaN</scp> Epitaxial Layer on Nonâ€Catalyticallyâ€grown Graphene. Bulletin of the Korean Chemical Society, 2016, 37, 1004-1009.	1.9	4
80	Strong enhancement of emission efficiency in GaN light-emitting diodes by plasmon-coupled light amplification of graphene. Nanotechnology, 2018, 29, 055201.	2.6	4
81	Possible permanent Dirac- to Weyl-semimetal phase transition by ion implantation. NPG Asia Materials, 2022, 14, .	7.9	4
82	Optical study of bulk and thin-film tin dioxide. Journal of the Korean Physical Society, 2012, 61, 2005-2010.	0.7	3
83	Sequential structural and optical evolution of MoS2 by chemical synthesis and exfoliation. Journal of the Korean Physical Society, 2015, 66, 1852-1855.	0.7	3
84	Blue-shifted and strongly-enhanced light emission in transition-metal dichalcogenide twisted heterobilayers. Npj 2D Materials and Applications, 2022, 6, .	7.9	3
85	Photoactive Deoxyribonucleic Acid (DNA) Bearing Carbazole Moieties and Its Photoluminescence Behavior With Ir(III) Complex. Molecular Crystals and Liquid Crystals, 2010, 519, 227-233.	0.9	2
86	Graphene synthesis from graphite/Ni composite films grown by sputtering. Journal of the Korean Physical Society, 2012, 61, 563-567.	0.7	2
87	High-performance Core/Shell InGaN/GaN Radial Multi-quantum-well Nanowire Solar Cells Non-catalytically Grown on Si Wafers. Journal of the Korean Physical Society, 2018, 73, 912-916.	0.7	2
88	Effect of Ge Concentration on the Temperature Dependence of Photoluminescence from Ge-Doped ZnO. Journal of the Korean Physical Society, 2008, 53, 426-430.	0.7	2
89	Effect of oxygen content on resistive switching memory characteristics of TiO x films. Journal of the Korean Physical Society, 2012, 60, 791-794.	0.7	1
90	Effect of Al concentration on the structural, electrical, and optical properties of transparent Al-doped ZnO. Journal of the Korean Physical Society, 2012, 61, 599-602.	0.7	1

#	Article	IF	CITATIONS
91	Formation properties of an InGaN active layer for high-efficiency InGaN/GaN multi-quantum-well-nanowire light-emitting diodes. Journal of the Korean Physical Society, 2016, 69, 772-777.	0.7	1
92	Non-catalytic direct synthesis of graphene on Si (111) wafers by using inductively-coupled plasma chemical vapor deposition. Journal of the Korean Physical Society, 2016, 69, 536-540.	0.7	1
93	Temperature-Dependent Carrier Recombination Processes in Nanocrystalline Si/SiO2 Multi-Layers Studied by Time-Resolved and Time-Integrated Photoluminescence. , 2006, , .		0
94	Characterization of Pd-nanocrystal-based nonvolatile memory devices. , 2006, , .		0
95	Blue-light emission from crystalline Si/silica core/shell nanowires. , 2008, , .		Ο
96	Effect of doping-induced defect concentration on the characteristics of Si-quantum-dot solar cells. , 2010, , .		0
97	Effect of defects in oxide templates on Non-catalytic growth of GaN nanowires for high-efficiency light-emitting diodes. Journal of the Korean Physical Society, 2016, 68, 864-868.	0.7	0